Available online at www.sciencedirect.com
SCIENCE DIRECT
International Journal of Heat and Mass Transfer 49 (2006) 4171–4182
International Journal of HEAT and MASS TRANSFER
www.elsevier.com/locate/ijhmt

Heat and mass transfer effectiveness and correlations for counter-flow absorbers

Md. Raisul Islam, N.E. Wijeysundera *, J.C. Ho

Department of Mechanical Engineering, National University of Singapore, 10 Kent Ridge Crescent, Singapore 119260, Singapore

Received 8 November 2005; received in revised form 23 March 2006
Available online 24 May 2006

Abstract

A simplified linear coupled heat and mass transfer model for counter-flow absorbers is validated by comparing its predictions with those of a numerical turbulent flow model. The simplified model lends itself to the formulation of a mass transfer effectiveness and a heat transfer effectiveness for counter-flow absorbers. The effectiveness is relatively insensitive to variations in the operating conditions of the absorber and depends mainly on the number of transfer units (NTU) and the capacity ratio. Available experimental data on a vertical tube absorber are analyzed using the simplified model to obtain heat and mass transfer correlations.

Keywords: Vapor absorption cooling; Turbulent falling-film absorbers; Mass transfer effectiveness; Heat transfer effectiveness; Numerical simulation

1. Introduction

Absorption cooling systems offer a viable alternative to vapor compression refrigeration cycles. The absorber is known to be the least efficient of all the sub-components of the absorption system due mainly to the relatively low rates of absorption of the refrigerant to the absorbent. Therefore much research and development effort has been devoted to the heat and mass transfer aspects of absorbers with a view to improving its performance. The absorption process that involves the coupled heat and mass transfer into a falling liquid film is difficult to model accurately. It is therefore desirable to develop simplified design models that are similar to the traditional effectiveness-NTU models used in heat exchanger design. Such models are useful in the analysis of experiments and the correlation of heat and mass transfer data. The present paper addresses these issues.

Models with varying complexity have been developed for the analysis of falling-film absorbers. These are discussed in detail in the review paper by Killon and Garimella [1]. Grossman [2] solved analytically the heat and mass diffusion equations in a falling film absorber. Ibrahim and Vinnicombe [3] presented a numerical model based on the finite difference method for a counter-flow absorber. Wekken and Wassenaar [4] solved the coupled heat and mass transfer equations using the finite element technique. Choudhury et al. [5] developed a numerical model for film flow over a horizontal round tube. The above papers considered falling films where the flow was in the laminar region. Grossman and Heath [6] and Yuksel and Schlunder [7] developed numerical models to analyze heat and mass transfer in a turbulent falling film. The latter compared the numerical predictions with their experimental data [8] and found these to be in good agreement. Patnaik and Perez-Blanco [9] developed numerical model to simulate the heat and mass transfer under wavy-laminar flow conditions.

There have been a number of efforts to develop simplified coupled models that are suitable for the design of absorbers. Patnaik and Perez-Blanco [10] and Patnaik et al. [11] developed simplified design approaches for absorbers by treating them as counter flow heat and mass exchangers. Conlisk [12] presented a design procedure for absorbers. Ryan [13] analyzed water absorption in an

* Corresponding author. Tel.: +65 874 2558; fax: +65 779 1459.
E-mail address: mpewijey@nus.edu.sg (N.E. Wijeysundera).

0017-9310/$ - see front matter © 2006 Elsevier Ltd. All rights reserved.
doi:10.1016/j.ijheatmasstransfer.2006.04.002

Nomenclature

a	constant in equilibrium relationship used in Eq. (8)
A	absorber area (m^2)
A_o	total area of absorber (m^2)
b	coefficient in equilibrium relationship used in Eq. (8) (K^{-1})
c_c	specific heat capacity of water ($J\,kg^{-1}\,K^{-1}$)
dQ_i	heat flow rate from solution to wall (W)
D	mass diffusivity ($m^2\,s^{-1}$)
Fr	Froude number $\frac{U_m^2}{g\delta}$
g	gravitational acceleration ($m\,s^{-2}$)
h_i	heat transfer coefficient from bulk solution to wall ($W\,m^{-2}\,K^{-1}$)
h_o	heat transfer coefficient from interface to bulk solution ($W\,m^{-2}\,K^{-1}$)
h_c	convective heat transfer coefficient for cooling water ($W\,m^{-2}\,K^{-1}$)
i_{ab}	enthalpy of absorption ($J\,kg^{-1}$)
i_{pw}	partial enthalpy of water at the interface ($J\,kg^{-1}$)
i_s	enthalpy of solution ($J\,kg^{-1}$)
i_v	enthalpy of water vapor at film interface ($J\,kg^{-1}$)
i_{vs}	difference in enthalpy ($J\,kg^{-1}$)
Ja	Jacobs number $\frac{bi_{ab}}{c_s}$
Ka	Kapitza number, $\frac{\sigma}{\rho_s(\nu^4 g)^{1/3}}$
k_{ef}	effective mass transfer coefficient from interface to bulk solution ($m\,s^{-1}$)
k_m	mass transfer coefficient from interface to bulk solution ($m\,s^{-1}$)
k_s	thermal conductivity of solution ($W\,m^{-1}\,K^{-1}$)
k_{wall}	thermal conductivity of tube wall ($W\,m^{-1}\,K^{-1}$)
L	length of absorber (m)
Le	Lewis number $\frac{\alpha}{D}$
m_{abs}	mass flux of vapor at film interface ($kg\,m^{-2}\,s^{-1}$)
Δm_s	vapor absorption rate ($kg\,s^{-1}$)
$\Delta m_{s,max}$	maximum vapor absorption rate ($kg\,s^{-1}$)
M_l	mass flow rate of LiBr ($kg\,s^{-1}$)
M_s	mass flow rate of solution ($kg\,s^{-1}$)
M_{sm}	mean mass flow rate of solution ($kg\,s^{-1}$)
m_c	mass flow rate of cooling water ($kg\,s^{-1}$)
Nu_i	Nusselt number $\frac{h_i(\nu^2/g)^{1/3}}{k_s}$
Nu_o	Nusselt number $\frac{h_o(\nu^2/g)^{1/3}}{k_s}$
P	absorber pressure (kPa)
P_o	reference pressure (kPa)
Pr	Prandtl number $\frac{\nu}{\alpha}$
Re	film Reynolds number $\frac{\Gamma}{\rho_s \nu}$
Sc	Schmidt number $\frac{\nu}{D}$
Sh_m	Sherwood number $\frac{k_m(\nu^2/g)^{1/3}}{D}$
T	temperature (°C)
U	solution velocity in X direction ($m\,s^{-1}$)
U_m	mean solution velocity in X direction ($m\,s^{-1}$)
U_{sc}	overall heat transfer coefficient from bulk solution to coolant ($W\,m^{-2}\,K^{-1}$)
V	solution velocity in Y direction ($m\,s^{-1}$)
We	Weber number $\frac{\rho_s \delta^2 g}{\sigma}$
X	coordinate in the direction of solution flow (m)
Y	coordinate in the direction of the film thickness (m)
Z	dimensionless variable used in Eq. (17)

Greek symbols

α	thermal diffusivity ($m^2\,s^{-1}$)
δ	film thickness (m)
δ_{wall}	wall thickness of absorber plate or tube (m)
ε_h	heat transfer effectiveness
ε_m	mass transfer effectiveness
ϕ	dimensionless variable used in Eq. (17)
φ	dimensionless variable used in Eq. (22)
λ	parameter
θ	dimensionless variable used in Eq. (17)
ρ	density ($kg\,m^{-3}$)
σ	surface tension (N/m)
ν	kinematic viscosity of solution ($m^2\,s^{-1}$)
ω	mass concentration of LiBr
ψ	dimensionless variable used in Eq. (22)
Γ	mass flow rate of solution per unit width of film ($kg\,m^{-1}\,s^{-1}$)

Subscripts

act	actual
c	coolant
e	equilibrium
ex	exit of absorber
if	solution–vapor interface
i	coolant inlet
max	maximum
o	entrance of absorber
s	solution
sb	bulk solution
t	turbulent
w	absorber wall

adiabatic spray of aqueous LiBr solution. Tsai and Perez-Blanco [14] and Andberg and Vliet [15] developed simplified models for falling-film absorbers. Uddholm and Settewall [16] used a model to predict the wave frequencies of the falling film.

Yuksel and Schlunder [8], Miller and Keyhani [17], Deng and Ma [18], Miller and Perez-Blanco [19] and Raisul et al. [20] among others conducted experimental investigations to obtain the heat and mass transfer coefficients for falling film absorbers. The correlation of the experimental

data could not be done in a consistent manner due to the unavailability of simplified design models [20]. A simplified model was developed and its predictions were validated for the laminar flow region by Raisul et al. [20,21].

In the present study the above model is extended for application to the turbulent flow region of the falling film. The simplified model yields closed form expressions of the heat and mass effectiveness of the absorber in terms of pertinent dimensionless variables. Published experimental data are analyzed using the simplified model to obtain the heat and mass transfer correlations for vertical tube absorbers.

2. Simplified model and absorber effectiveness

2.1. Simplified model and dimensionless parameters

The counter-flow absorber is represented schematically as shown in Fig. 1. The energy balance for a small control volume in the coolant flow gives

$$\frac{dT_c}{dA} = -\left(\frac{U_{sc}}{m_c c_c}\right)(T_{sb} - T_c) \tag{1}$$

The overall heat transfer coefficient is

$$\frac{1}{U_{sc}} = \frac{1}{h_c} + \frac{1}{h_i} + \frac{\delta_{wall}}{k_{wall}} \tag{2}$$

The heat transfer coefficients are suitably scaled to have the same heat transfer area.

The mass conservation equation for the solution is

$$\frac{dM_s}{dA} = k_m \rho_s (\omega_{sb} - \omega_{if}) \tag{3}$$

The driving potential for mass transfer [22] has been linearized because the variation of ω_{if} is relatively small compared to that of $(\omega_{sb} - \omega_{if})$.

Expressing the enthalpy of the solution as a linear function of the temperature and concentration over the narrow range of operation of practical absorbers, the energy equation for the solution may be written as:

$$M_s c_s \frac{dT_{sb}}{dA} + M_s c_w \frac{d\omega_{sb}}{dA} = (i_v - i_s)\frac{dM_s}{dA} - U_{sc}(T_{sb} - T_c) \tag{4}$$

The coefficients on the LHS of the above equation are given by

$$c_s = \left[\frac{\partial i_s}{\partial T_{sb}}\right]_{\omega_{sb}} \quad \text{and} \quad c_w = \left[\frac{\partial i_s}{\partial \omega_{sb}}\right]_{T_{sb}} \tag{5}$$

The liquid–vapor interface condition is obtained by applying the energy equation to an infinitesimally thin control volume enclosing the interface. This gives

$$m_{abs} i_v dA = m_{abs} i_{pw} dA + h_o (T_{if} - T_{sb}) dA \tag{6}$$

where $(m_{abs}\,dA)$ is a mass of water absorbed at the interface. i_{pw} is the partial enthalpy of the absorbed water at the interface, which is a function of interface temperature and concentration [2]. Since water mass conservation gives, $m_{abs} = dM_s/dA$, Eq. (6) can be rearranged using Eq. (3) in the form

$$k_m \rho_s (\omega_{sb} - \omega_{if}) i_{ab}\, dA = h_o (T_{if} - T_{sb})\, dA \tag{7}$$

where $i_{ab} = (i_v - i_{pw})$, is the enthalpy of absorption in the liquid. The vapor enthalpy i_v at the interface is a function of the interface temperature and the absorber pressure. For the range of interface temperature changes encountered in practical systems (Fig. 2) the variation of $(i_v - i_{pw}) = i_{ab}$ is about 0.8%. Therefore, in the present simplified model the value of i_{ab} was evaluated at the mean temperature.

The vapor–liquid interface is assumed to be at equilibrium corresponding to the pressure of the system. Assuming the equilibrium condition to be linear [3]

$$\omega_{if} = a + bT_{if} \tag{8}$$

The constants a and b are functions of the absorber pressure. For the practically relevant pressure range of 0.8 kPa to 2 kPa for LiBr-water systems, these constants are well represented by the expressions

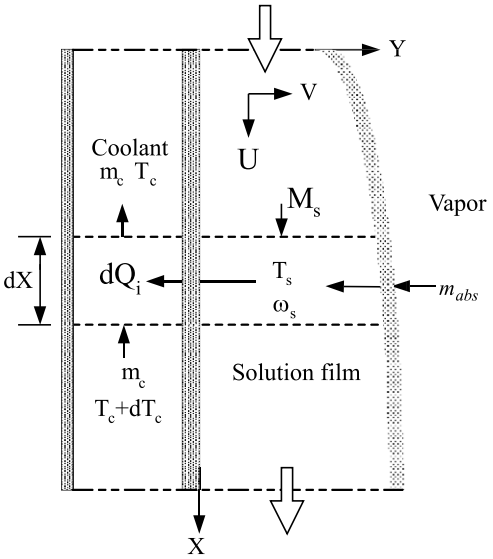

Fig. 1. Physical model for numerical simulation.

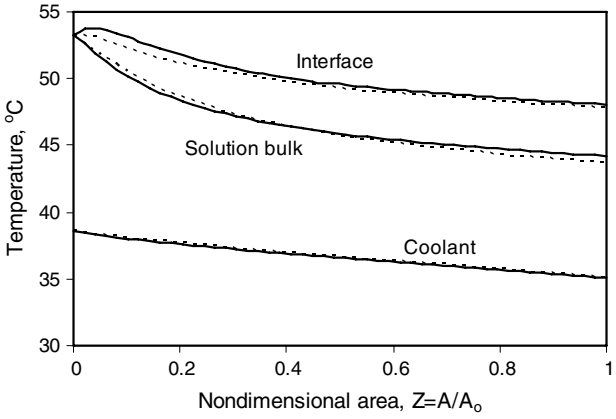

Fig. 2. Temperature distribution within absorber. Graphs: (——) Turbulent model, (------) simplified model.

$$a = 0.37794\left(\frac{P}{P_o}\right)^{-0.188} \quad \text{and}$$

$$b = 4.8688 \times 10^{-3}\left(\frac{P}{P_o}\right)^{-0.06574} \tag{9}$$

where P is the absorber pressure in kPa and P_o is the reference pressure taken as 1.0 kPa.

From Eqs. (7) and (8), the interface concentration becomes

$$\omega_{if} = \frac{\lambda(a + bT_{sb}) + b\omega_{sb}}{(\lambda + b)} \tag{10}$$

where $\lambda = \dfrac{h_o}{i_{ab}k_m\rho_s}$.

Substituting for ω_{if} from Eq. (10) in Eq. (3), the solution mass conservation equation takes the form

$$\frac{dM_s}{dA} = k_{ef}\rho_s[\omega_{sb} - (a + bT_{sb})] \tag{11}$$

where the effective mass transfer coefficient is defined as

$$\frac{1}{k_{ef}} = \frac{1}{k_m} + \frac{bi_{ab}\rho_s}{h_o} \tag{12}$$

Since the mass flow rate of the absorbent in the solution is constant

$$M_s = \frac{M_1}{\omega_{sb}} \tag{13}$$

Differentiating Eq. (13)

$$\frac{d\omega_{sb}}{dA} = -\left[\frac{M_1}{M_s^2}\right]\left[\frac{dM_s}{dA}\right] \tag{14}$$

Substituting in Eq. (11) from Eq. (14)

$$\frac{d\omega_{sb}}{dA} = -k_{ef}\rho_s\left[\frac{M_1}{M_s^2}\right][\omega_{sb} - (a + bT_{sb})] \tag{15}$$

Substituting from Eqs. (11) and (15) in Eq. (4) becomes

$$\frac{dT_{sb}}{dA} = k_{ef}\rho_s\left(\frac{i_{vs}}{M_s c_s} + \frac{c_w M_1}{c_s M_s^2}\right)[\omega_{sb} - (a + bT_{sb})] - \left(\frac{U_{sc}}{M_s c_s}\right)(T_{sb} - T_c) \tag{16}$$

where $i_{vs} = (i_v - i_s)$.

Two additional assumptions are introduced for the purpose of making the governing Eqs. (15) and (16) linear. The mass flow rate of the solution is assumed constant at the mean value, M_{sm} and all the other property values that occur in the coefficients of the above equations are assumed constant at their mean values.

2.1.1. Dimensionless groups and solution

The governing equations (1), (15) and (16) are cast in dimensionless form by substituting the following dimensionless variables for temperature, concentration and area:

$$\theta = \frac{T - T_{s,o}}{\Delta T}, \quad \phi = \frac{\omega - \omega_{s,o}}{\Delta\omega} \tag{17}$$

where $\Delta T = \dfrac{(\omega_{s,o} - a)}{b} - T_{s,o}$ and $\Delta\omega = (a + bT_{s,o}) - \omega_{s,o}$.

$Z = \dfrac{A}{A_o}$ where A_o is the total heat transfer area of the absorber.

Manipulating Eq. (17)

$$\frac{\omega_e - \omega_{s,o}}{T_e - T_{s,o}} = \frac{\Delta\omega}{\Delta T} = -b \tag{18}$$

When the dimensionless variables are substituted in the governing equations (1), (15) and (16), the following equations are obtained:

$$\frac{d\theta_c}{dZ} = -\left(\frac{U_{sc}A_o}{m_c c_c}\right)(\theta_{sb} - \theta_c) \tag{19}$$

$$\frac{d\phi_{sb}}{dZ} = -A_o k_{ef}\rho_s\left[\frac{M_1}{M_{sm}^2}\right][\phi_{sb} + \theta_{sb} - 1] \tag{20}$$

$$\frac{d\theta_{sb}}{dZ} = -A_o k_{ef}\rho_s\left(\frac{bi_{vs}}{M_{sm}c_s} + \frac{bc_w M_1}{c_s M_{sm}^2}\right)[\phi_{sb} + \theta_{sb} - 1] - \left(\frac{A_o U_{sc}}{M_{sm}c_s}\right)(\theta_{sb} - \theta_c) \tag{21}$$

Eqs. (19)–(21) can be reduced to two coupled equations by defining two new dimensionless variables. These are

$$\psi = 1 - \phi_{sb} - \theta_{sb} \quad \text{and} \quad \varphi = \theta_{sb} - \theta_c \tag{22}$$

Substituting in Eqs. (1) and (3) it can be shown that φ and ψ are the driving potentials for the heat flux and mass flux respectively.

When expressed in terms of the above variables Eqs. (19)–(21) become

$$\frac{d\varphi}{dZ} = \left(\frac{A_o k_{ef}\rho_s}{M_{sm}}\right)\left(\frac{bi_{vs}}{c_s} + \frac{bc_w M_1}{c_s M_{sm}}\right)\psi - \left(\frac{A_o U_{sc}}{M_{sm}c_s}\right)\left(1 - \frac{M_{sm}c_s}{m_c c_c}\right)\varphi \tag{23}$$

$$\frac{d\psi}{dZ} = -\left(\frac{A_o k_{ef}\rho_s}{M_{sm}}\right)\left(\frac{bi_{vs}}{c_s} + \frac{bc_w M_1}{c_s M_{sm}} + \frac{M_1}{M_{sm}}\right)\psi + \left(\frac{A_o U_{sc}}{M_{sm}c_s}\right)\varphi \tag{24}$$

Eqs. (23) and (24) are two coupled linear differential equations in which the coefficients are functions of six dimensionless groups. These are as follows

$$\pi_1 = \left(\frac{A_o k_{ef}\rho_s}{M_{sm}}\right); \quad \pi_2 = \left(\frac{A_o U_{sc}}{M_{sm}c_s}\right); \quad \pi_3 = \left(\frac{M_{sm}c_s}{m_c c_c}\right); \quad \pi_4 = \left(\frac{bi_{vs}}{c_s}\right); \quad \pi_5 = \left(\frac{bc_w}{c_s}\right) \quad \text{and} \quad \pi_6 = \left(\frac{M_1}{M_{sm}}\right) \tag{25}$$

Comparing with traditional heat exchanger analysis, the variables π_1 and π_2 are the number of transfer units (NTU) for mass transfer and heat transfer respectively and π_3 is the capacity ratio. π_4 and π_5 are ratios of the latent enthalpy to the sensible heat of the solution, which is similar to the inverse of the Jakob number [17] while π_6 is essentially the mean concentration of the solution.

The overall heat and mass transfer coefficients U_{sc} and k_{ef} are related to the basic transfer coefficients through the relations (2) and (12) respectively. When these are expressed in dimensionless form, π_1 and π_2 can be written in terms of three additional dimensionless groups.

$$\frac{1}{\pi_1}=\frac{1}{\pi_7}+\frac{\pi_9}{\pi_8} \quad \text{and} \quad \frac{1}{\pi_2}=\frac{\pi_3}{\pi_{10}}+\frac{1}{\pi_{11}} \tag{26}$$

where $\pi_7=\dfrac{A_o k_m \rho_s}{M_{sm} c_s}$; $\pi_8=\dfrac{A_o h_o}{M_{sm} c_s}$; $\pi_9=\dfrac{b i_{ab}}{c_s}$;

$$\pi_{10}=\frac{A_o h_w}{M_w c_w} \quad \text{and} \quad \pi_{11}=\frac{A_o h_i}{M_{sm} c_s} \tag{27}$$

For the purpose of obtaining an analytical solution, (23) and (24) are expressed in the compact form

$$\frac{d\varphi}{dZ}=g_1\psi+g_2\varphi \tag{28}$$

$$\frac{d\psi}{dZ}=g_3\varphi+g_4\psi \tag{29}$$

where the coefficients are given by:

$$g_1=\pi_1(\pi_4+\pi_5\pi_6); \quad g_2=\pi_2(\pi_3-1)$$
$$g_3=\pi_2 \quad \text{and} \quad g_4=-\pi_1(\pi_4+\pi_5\pi_6+\pi_6) \tag{30}$$

The solution of (28) and (29) are obtained using the Laplace Transformation technique. The final forms of the solutions are as follows

$$\varphi(Z)=a_1 e^{\alpha_1 Z}+a_2 e^{\alpha_2 Z} \tag{31}$$

$$\text{and} \quad \psi(Z)=b_1 e^{\alpha_1 Z}+b_2 e^{\alpha_2 Z} \tag{32}$$

where the roots of the characteristic equation are

$$\alpha_1,\alpha_2=0.5(g_2+g_4)\pm 0.5[(g_2+g_4)^2-4(g_2g_4-g_1g_3)]^{1/2} \tag{33}$$

The coefficients are given by:

$$a_1=\frac{\varphi_o(\alpha_1-g_4)+\psi_o g_1}{\alpha_1-\alpha_2} \tag{34}$$

$$a_2=\frac{\varphi_o(\alpha_2-g_4)+\psi_o g_1}{\alpha_2-\alpha_1} \tag{35}$$

$$b_1=\frac{\psi_o(\alpha_1-g_2)+\varphi_o g_3}{\alpha_1-\alpha_2} \tag{36}$$

$$b_2=\frac{\psi_o(\alpha_2-g_2)+\varphi_o g_3}{\alpha_2-\alpha_1} \tag{37}$$

where φ_o and ψ_o are the values at $Z=0$. From Eqs. (17) and (22) it follows that

$$\psi_o=1 \quad \text{and} \quad \varphi_o=-\theta_{co} \tag{38}$$

where θ_{co} is the coolant exit temperature.

2.2. Effectiveness of absorber

The absorber is essentially a mass and heat transfer device. Therefore it is useful to characterize its performance using the concept of a mass transfer effectiveness and a heat transfer effectiveness. For a counter-flow arrangement the maximum mass absorption rate will occur in an ideal device where the solution is cooled to the inlet temperature of the coolant. The solution concentration will then attain the equilibrium concentration corresponding to the coolant inlet temperature. Because the solution is cooled to the inlet temperature of the coolant, the heat transfer to the coolant under these conditions may be assumed the maximum. Patnaik and Perez-Blanco [10] used the same definition for the effectiveness in their simplified model.

2.2.1. Mass transfer effectiveness

Since the proposed effectiveness is to be based on the foregoing simplified model all quantities needed for the evaluation of the effectiveness are obtained using the appropriate equations of the model.

The total mass absorption rate is obtained by rearranging Eq. (14) in the form

$$\frac{dM_s}{dA}=-\left(\frac{M_{sm}^2}{M_1}\right)\frac{d\omega_{sb}}{dA} \tag{39}$$

The mass absorption rate is found by integrating (39) from inlet to outlet of the absorber

$$\Delta m_s=-\left(\frac{M_{sm}^2}{M_1}\right)(\omega_{s,ex}-\omega_{s,o})=-\frac{M_{sm}\phi_{sb,ex}\Delta\omega}{\pi_6} \tag{40}$$

When the mass absorption rate is a maximum, solution at exit of the absorber is saturated at the inlet coolant temperature. Then the dimensionless concentration at exit is

$$\phi_{sb,ex}=\frac{(a+bT_{ci})-\omega_{s,o}}{\Delta\omega}=1-\theta_{ci} \tag{41}$$

Substituting in (40) the maximum rate of mass absorption is

$$\Delta m_{s,max}=-\frac{M_{sm}(1-\theta_{ci})\Delta\omega}{\pi_6} \tag{42}$$

Using (40) and (42), the mass transfer effectiveness can be written as

$$\varepsilon_m=\frac{\Delta m_s}{\Delta m_{s,max}}=\frac{\phi_{ex}}{(1-\theta_{ci})} \tag{43}$$

From Eq. (22) it follows that, in general

$$\phi_{sb,ex}=(1-\theta_{ci})-(\varphi_{ex}+\psi_{ex}) \tag{44}$$

$$\text{and} \quad \theta_{sb,ex}=\theta_{ci}+\varphi_{ex} \tag{45}$$

Substituting in (43) from (44)

$$\varepsilon_m=1-\frac{(\varphi_{ex}+\psi_{ex})}{(1-\theta_{ci})} \tag{46}$$

From Eqs. (41) and (44) when the maximum absorption rate occurs, $(\varphi_{ex}+\psi_{ex})=0$ and from Eq. (46), $\varepsilon_m\to 1$. The variables φ_{ex} and ψ_{ex} are the driving potentials for heat transfer and mass transfer at the exit of the absorber. As seen from (46) the effectiveness increases as these potentials at the exit decrease and eventually approaches unity as the potentials approach zero for the ideal absorber.

Substituting from Eqs. (31) and (32) in Eq. (46)

$$\varepsilon_m = 1 - \frac{(b_1 + a_1)e^{\alpha_1} + (b_2 + a_2)e^{\alpha_2}}{(1 - \theta_{ci})} \tag{47}$$

Substituting for the coefficients from Eqs. (34)–(37) the final form of the mass transfer effectiveness becomes

$$\varepsilon_m = 1 - \frac{(1-\theta_{co})(\alpha_1 e^{\alpha_1} - \alpha_2 e^{\alpha_2}) + [g_1 - g_2 - \theta_{co}(g_3 - g_4)](e^{\alpha_1} - e^{\alpha_2})}{(1-\theta_{ci})(\alpha_1 - \alpha_2)} \tag{48}$$

The coefficients in Eq. (48) are in terms of the coolant temperature at the entrance, $Z = 0$. Being a counter-flow absorber the coolant temperature is known only at the exit of the absorber. The relation between the inlet and out coolant temperatures is obtained by integrating (19). Therefore

$$\theta_{co} - \theta_{ci} = \pi_2 \int_0^1 \varphi \, dZ = \pi_3 \pi_2 \int_0^1 \left(a_1 e^{\alpha_1 Z} + a_2 e^{\alpha_2 Z}\right) dZ \tag{49}$$

On simplification of Eq. (49) after substituting for the coefficients from Eqs. (34) and (35) the exit coolant temperature becomes

$$\theta_{co} = \frac{\theta_{ci}\alpha_1\alpha_2(\alpha_1 - \alpha_2) + \pi_3\pi_2 g_1(\alpha_2 e^{\alpha_1} - \alpha_1 e^{\alpha_2}) + \pi_3\pi_2 g_1(\alpha_1 - \alpha_2)}{\alpha_1\alpha_2(\alpha_1 - \alpha_2) + \pi_3\pi_2\alpha_1\alpha_2(e^{\alpha_1} - e^{\alpha_2}) - \pi_3\pi_2 g_4(\alpha_2 e^{\alpha_1} - \alpha_1 e^{\alpha_2}) - \pi_3\pi_2 g_4(\alpha_1 - \alpha_2)} \tag{50}$$

The mass transfer effectiveness is evaluated by first computing the exit coolant temperature using Eq. (50) and substituting the resulting value in Eq. (48).

2.2.2. Heat transfer effectiveness

The heat transfer effectiveness is defined as

$$\varepsilon_h = \frac{Q_{act}}{Q_{max}} = \frac{m_c c_c(\theta_{co} - \theta_{ci})}{m_c c_c\ (\theta_{cm} - \theta_{ci})} \tag{51}$$

where θ_{cm} is the dimensionless coolant outlet temperature when outlet solution temperature is equal to the coolant inlet temperature. The expression Eq. (51) for the heat transfer effectiveness is evaluated by combining Eqs. (1), (4) and (14) to give the differential form

$$\left(\frac{m_c c_c}{M_{sm} c_s}\right)\frac{dT_c}{dA} = \frac{dT_{sb}}{dA} + \left(\frac{i_{vs}}{M_{sm} c_s} + \frac{c_w M_1}{c_s M_{sm}^2}\right)\left(\frac{M_{sm}^2}{M_1}\right)\frac{d\omega_{sb}}{dA} \tag{52}$$

When expressed in terms of the dimensionless variables Eq. (52) becomes

$$\frac{d\theta_c}{dZ} = \pi_3 \frac{d\theta_{sb}}{dZ} - \frac{\pi_3(\pi_5\pi_6 + \pi_4)}{\pi_6}\frac{d\phi_{sb}}{dZ} \tag{53}$$

Integrating Eq. (53) from inlet to the exit of the absorber and noting that at $Z = 0$, $\theta_{sb}(0) = \phi_{sb}(0) = 0$

$$\theta_{ci} - \theta_{co} = \pi_3 \theta_{sb,ex} - \frac{\pi_3(\pi_5\pi_6 + \pi_4)\phi_{sb,ex}}{\pi_6} \tag{54}$$

The actual heat transfer is given by

$$Q_{act} = m_c c_c(\theta_{co} - \theta_{ci})\Delta T = m_c c_c \Delta T \pi_3 \left[\frac{(\pi_5\pi_6 + \pi_4)\phi_{sb,ex}}{\pi_6} - \theta_{sb,ex}\right] \tag{55}$$

When the maximum heat transfer rate occurs,

$$\theta_{sb,ex} = \theta_{ci} \quad \text{and from Eq. (22)} \quad \phi_{sb,ex} = 1 - \theta_{ci} \tag{56}$$

The maximum heat transfer rate is given by

$$Q_{max} = m_c c_c(\theta_{cm} - \theta_{ci})\Delta T = m_c c_c \Delta T \pi_3 \left[\frac{(\pi_5\pi_6 + \pi_4)(1 - \theta_{ci})}{\pi_6} - \theta_{ci}\right] \tag{57}$$

Substituting in Eq. (51)

$$\varepsilon_h = \frac{(\pi_5\pi_6 + \pi_4)\phi_{sb,ex} - \pi_6\theta_{sb,ex}}{(\pi_5\pi_6 + \pi_4)(1 - \theta_{ci}) - \pi_6\theta_{ci}} \tag{58}$$

Substituting from Eq. (56) for $\phi_{sb,ex}$ and $\theta_{sb,ex}$

$$\varepsilon_h = 1 - \frac{(\pi_5\pi_6 + \pi_4)(\varphi_{ex} + \psi_{ex}) + \pi_6\varphi_{ex}}{(\pi_5\pi_6 + \pi_4)(1 - \theta_{ci}) - \pi_6\theta_{ci}} \tag{59}$$

It is seen from Eq. (59) that as in the case of ε_m, ε_h increases as the driving potentials φ_{ex} and ψ_{ex} at the absorber exit decreases and eventually approaches unity when the potentials approach zero for the ideal absorber.

Substituting from Eqs. (44) and (45) for the φ_{ex} and ψ_{ex} the effectiveness becomes

$$\varepsilon_h = 1 - \frac{(\pi_5\pi_6 + \pi_4)[(a_1 + b_1)e^{\alpha_1} + (a_2 + b_2)e^{\alpha_2}] + \pi_6(a_1 e^{\alpha_1} + a_2 e^{\alpha_2})}{(\pi_5\pi_6 + \pi_4)(1 - \theta_{ci}) - \pi_6\theta_{ci}} \tag{60}$$

The heat transfer effectiveness is evaluated by substituting in Eq. (60) for the coefficients from Eqs. (34)–(37) and θ_{co} from Eq. (50).

2.2.3. Turbulent falling film model

One of the objectives of the present study is to extend the application of the simplified model to the turbulent flow regime of the falling film. Therefore a turbulent heat and mass transfer model similar in all respects to that presented by Yuksel and Schlunder [7] was developed for comparison with the simplified model. The main equations of the turbulent and the solution procedure are summarized in the Appendix. For the sake of brevity, the reader is referred to the paper by Yuksel and Schlunder [7] for additional details of the formulation and computational procedures.

2.2.4. Heat and mass transfer correlations

The use of the simplified model and the computation of the effectiveness require the relevant heat and mass transfer coefficients which has to be extracted from experimental data. The published experimental data of Miller [23] was selected for this purpose due to the availability of all required information in tabular form. The experiments were carried out with water cooled vertical tube absorber of outer diameter 0.019 m and effective length 1.52 m. Details of the experimental procedure and data analysis are also available in Miller and Keyhani [17].

The values of U_{sc} and k_{ef} were obtained for each test run by substituting the inlet and outlet conditions in Eqs. (31) and (32) and solving the resulting non-linear equations. An optimization routine that minimizes the sum of the error-square between the predicted and measured changes in coolant temperature, solution temperature and concentration across the absorber was found to be the most convenient and accurate procedure to extract the values U_{sc} and k_{ef}. When the original experimental data has been appropriately conditioned, as was done by Miller [23], to ensure exact energy and mass balance, the solution converges rapidly to yield unique values for U_{sc} and k_{ef}. The heat transfer coefficient from the bulk fluid to the tube wall h_i is obtained by substituting for h_w and the tube wall resistance in Eq. (2). The former was computed using the correlations give by Miller [23]. The resulting values of h_i are correlated using a relation of the form $Nu_i = cRe^nPr^m$.

The separation of the individual transfer coefficients h_o and k_m from the extracted values of k_{ef} involves some uncertainty. In the present work, the heat and mass transfer processes from the interface to the bulk fluid are assumed to satisfy the heat and mass transfer analogy. This was demonstrated experimentally by Yuksel and Schlunder [8] for turbulent film flow by measuring the interface temperature of the film. Therefore as a first attempt at obtaining a correlation the following relations are assumed.

$$Nu_o = cRe^nPr^m \quad \text{and} \quad Sh_m = cRe^nSc^m \tag{61}$$

From Eq. (61) it follows that

$$\frac{h_o}{k_m} = c_s\rho_s Le^{(1-m)} \tag{62}$$

Substituting the above relation in Eq. (12)

$$k_m = k_{ef}[1 + (i_{ab}b/c_s)Le^{(m-1)}] \tag{63}$$

where Le is the Lewis number and the ratio (c_s/bi_{ab}) is the Jakob number.

The results of applying these correlations to the experimental data of Miller [23] will be discussed in the next section.

3. Results and discussion

The temperature and concentration distributions predicted by the turbulent model and the simplified model with U_{sc} and k_{ef} values obtained from the former are shown in Figs. 2 and 3. There is, in general, good agreement between the predictions of the simplified linear model and the turbulent model with only a small deviation in the interface concentration. This is presumably, due to the linearised mass transfer driving potential used in the simplified model in contrast to the non-linear interface boundary condition Eq. (A.27) used in the turbulent model. From these comparisons it can be concluded that the simplified model with appropriate heat and mass transfer coefficients may be used to model absorbers with turbulent film flow. Similar conclusion was reached by Raisul et al. [21] using laminar film flow conditions in counter flow absorbers.

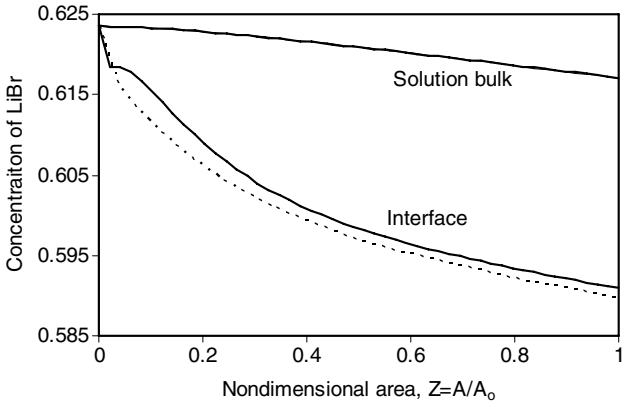

Fig. 3. Concentration distribution within absorber. Graphs: (——) Turbulent model, (------) simplified model.

3.1. Effectiveness of the absorber

The mass transfer effectiveness ε_m and the heat transfer effectiveness ε_h are convenient performance parameters that may be used in design. However, it evident from Eqs. (48) and (60) that ε_m and ε_h depend on seven dimensionless quantities π_1 to π_6 and θ_{ci}. A sensitivity study was carried out to identify the parameters on which the effectiveness depends strongly. The data in Table 1 shows that both ε_m and ε_h are relatively insensitive to changes in π_4 to

Table 1
Effect of dimensionless operating variables on effectiveness

Parameters varied	Range	ε_m	ε_h
$\pi_4 = \left(\frac{bi_{vs}}{c_s}\right)$	6.0	0.32	0.36
	7.0	0.30	0.33
$\pi_5 = \left(\frac{bc_w}{c_s}\right)$	−2.0	0.32	0.37
	−1.0	0.31	0.35
$\pi_6 = \left(\frac{M_1}{M_{sm}}\right)$	0.57	0.30	0.34
	0.64	0.33	0.37
$\theta_{w,in} = \frac{T_{w,in} - T_{s,o}}{T_e - T_{s,o}}$	−32.0	0.32	0.35
	0.15	0.35	0.31

Design variables $\pi_1 = 1.5$, $\pi_2 = 15.0$, $\pi_3 = 0.15$.

π_6 and θ_{ci} in the general range of values of these parameters applicable to practical absorbers. It is noteworthy that π_6 is essentially the average concentration of the solution and θ_{ci} is dimensionless coolant inlet temperature which is a function of the inlet solution temperature and concentration and the inlet coolant temperature. Moreover, these are all operating conditions of the absorber. The parameters π_4 and π_5 are dependent on the properties of the solution while the value of b varies with the absorber pressure. The effectiveness does not vary markedly with the changes in these parameters as seen from the data in Table 1.

In the case of traditional heat exchanger analysis the expressions for the effectiveness are completely independent of the operating temperatures of the two fluids. However, for absorbers the respective expressions (48) and (60) for ε_m and ε_h appear to depend explicitly on the operating conditions. Nevertheless, the relative insensitivity of ε_m and ε_h to the operating conditions of the absorber in the range of values encountered in practice makes the effectiveness an acceptable performance parameter for the design of absorbers.

As anticipated, the main dimensionless design variables on which the effectiveness depends are π_1, π_2 and π_3. It is seen that π_1 and π_2 are the number of transfer units (NTU) for mass and heat transfer respectively and π_3 is the capacity ratio. The variation of the effectiveness with these important design parameters is shown in Figs. 4–7 where the general trend of the curves is similar to that for counter-flow heat exchangers. Although the plots are useful to depict the trends, the values of the effectiveness are easily computed using analytical expressions (48), (50) and (60). It is interesting to note that the maximum mass and heat transfer rates given by expressions (42) and (57) respectively depend on the fluid flow rates, the fluid properties and the operating conditions as in the case of a conventional heat exchanger. Therefore these quantities could be calculated readily and multiplied by the respective effectiveness to obtain the actual mass and heat transfer rates.

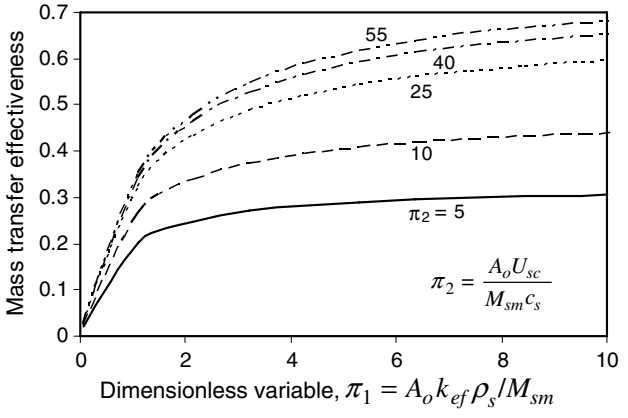

Fig. 4. Variation of mass transfer effectiveness with π_1 for different values of π_2.

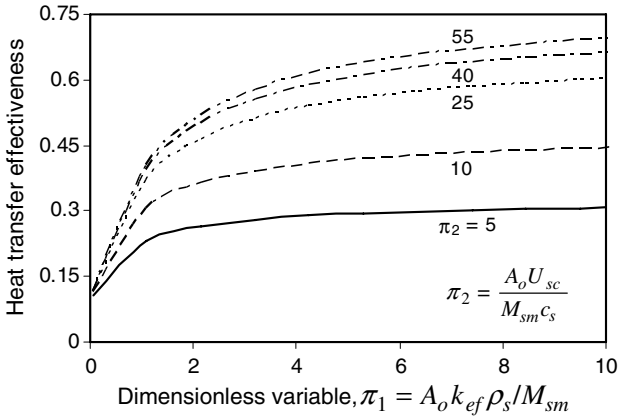

Fig. 5. Variation of heat transfer effectiveness with π_1 for different values of π_2.

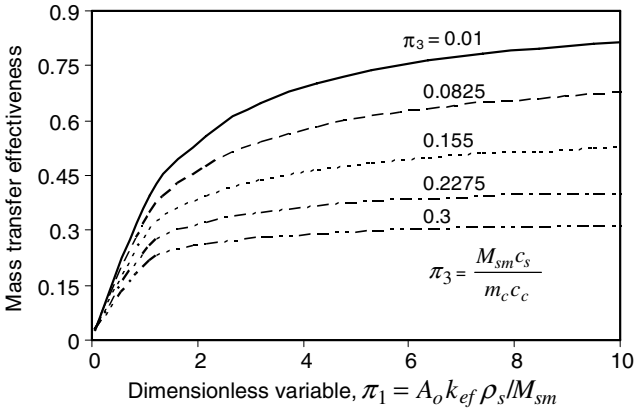

Fig. 6. Variation of mass transfer effectiveness with π_1 for different values of π_3.

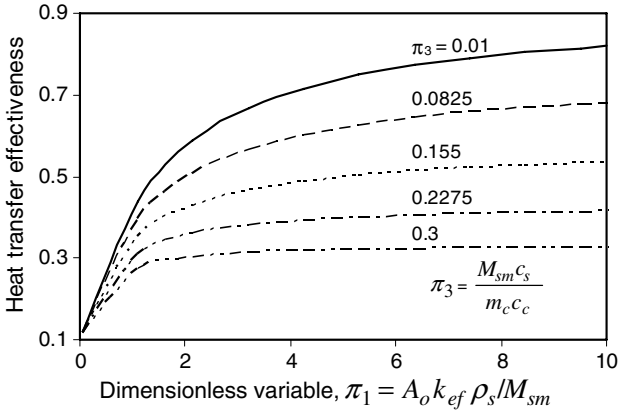

Fig. 7. Variation of heat transfer effectiveness with π_1 for different values of π_3.

3.2. Heat and mass transfer correlations

The 26 data sets tabulated by Miller [23] covered a pressure range of 1.17–1.52 kPa, a LiBr-solution flow rate of 0.25–0.42 kg m^{-1} s^{-1} and a coolant inlet temperature of about 35 °C. The heat and mass transfer coefficients were

extracted from the test data using the procedure described in Section 2 above. The heat transfer coefficient h_i from the bulk solution to the tube wall was on the average about 1050 $Wm^{-2}K^{-1}$ and it varied only about 10% for all the runs. The flow regimes for the test runs have been identified as wavy-laminar to wavy-transition with a submerged layer underneath the wavy surface. The relative insensitivity of h_i to the experimental conditions may be due to the presence of this submerged layer.

In contrast, the effective mass transfer coefficient, k_{ef} was found to vary about 50% between the various test runs. k_{ef} was decomposed in to the respective mass and heat transfer coefficients k_m and h_o using Eqs. (62) and (63) with an exponent of 0.4–0.5 for the Schmidt and Prandtl numbers as obtained experimentally by Yuksel and Schlunder [8]. The value of h_o thus calculated varied from about 1650 to 3050 $Wm^{-2}K^{-1}$ while the range of k_m was from about 4.1×10^{-5} to 7.7×10^{-5} m s^{-1}. Extensive exploratory efforts showed that the relations (61) was not adequate to correlate the data for h_o and k_m in a satisfactory manner. Therefore additional dimensionless groups like the Kapitza number had to be introduced. The extracted value of k_{ef} showed marked sensitivity to the parameter b in the equilibrium relation (8). For instance, when all other input data are held constant, a change of 2% in the value of a resulted in a change of about 25% in the value of k_{ef}. For a 2% change in the value of b the corresponding change in k_{ef} is about 20%. This is because the driving potential for mass transfer, ψ depends markedly on the values of a and b, which in turn are dependent on the absorber pressure as seen from Eq. (9).

It was therefore decided to introduce the pressure parameter, $\frac{P}{P_o}$ directly to the final form of the correlation for both the Sherwood and Nusselt numbers. Yang and Jou [24] correlated their heat and mass transfer data for wavy film absorption using a similar pressure ratio. The exponent in their case was about 1.5 to 1.7 while the exponent in the present study is about 1.3. The correlations thus obtained are given in Table 2 with range of the different dimensionless variables. A comparison of the experimentally extracted values with those predicted by the correlations is shown in Figs. 8–10. The root-mean-deviation for Nu_i is 4.2% while for Nu_o and Sh_m it is about 9.2%. Although the range of application of the correlations obtained is limited by the experimental data considered in the present work, the results obtained has demonstrated the feasibility of using the simplified model for the analysis and correlation of experimental data on absorbers.

Table 2
Heat and mass transfer correlations

Correlations
$Nu_i = 0.138\ Re^{-0.132}Pr^{0.351}$
$Nu_o = 1.064\times10^{-3}\ Re^{-0.093}Pr^{0.45}\ Ja^{0.55}Ka^{0.6}(P/P_o)^{1.3}$
$Sh_m = 1.064\times10^{-3}\ Re^{-0.093}\ Sc^{0.45}Ja^{0.55}Ka^{0.6}(P/P_o)^{1.3}$
Range
$Re = 50$–95; $Sc = 1800$–2200
$Pr = 20$–23; $Ja = 4$–6; $Ka = 550$–650

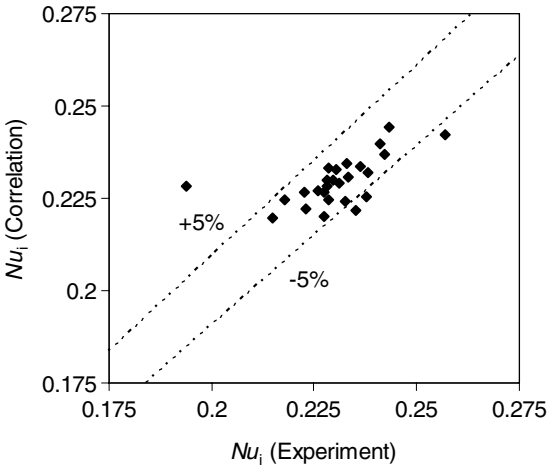

Fig. 8. Comparison of experimental and predicted Nusselt number, Nu_i.

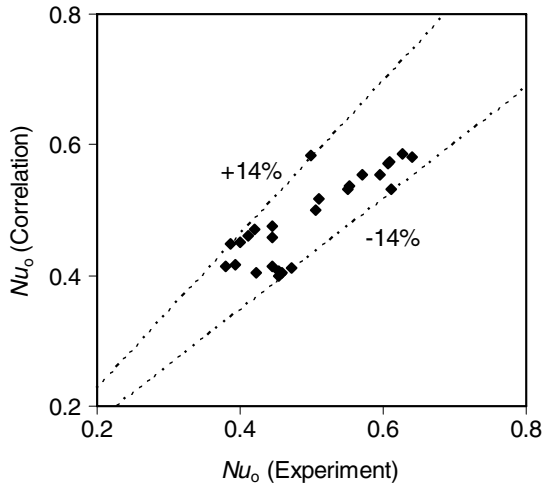

Fig. 9. Comparison of experimental and predicted Nusselt number, Nu_o.

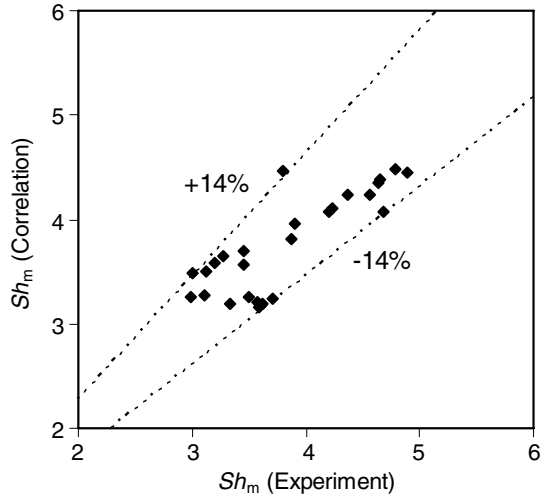

Fig. 10. Comparison of experimental and predicted Sherwood number, Sh_m.

4. Conclusion

Overall heat and mass transfer coefficients obtained from a turbulent film flow model were used in a simplified model to predict the distributions of the fluid temperatures and concentrations in the absorber. These were in good agreement with the corresponding distributions produced by the turbulent model thus lending credence to the simplified model. A heat transfer effectiveness and a mass transfer effectiveness for the absorber was formulated by extending the simplified model. The effectiveness was relatively insensitive to variations of the operating conditions of the absorber in the range encountered in practice. As in heat exchangers, the effectiveness of the absorber was mainly dependent on the mass and heat transfer-NTU and the capacity ratio of the fluids. Heat and mass transfer correlations were developed for the pertinent heat and mass transfer coefficients that are needed as input for computations with the simplified model and the absorber effectiveness.

Appendix A. Turbulent model for falling film

In the physical model shown schematically in Fig. 1, a thin film of strong LiBr-solution flows down over a vertical flat plate. The film is in contact with stagnant water vapor at constant pressure.

The following assumptions are made in developing the turbulent numerical model:

1. Eddy transport coefficients added to the molecular diffusivities for momentum, thermal and mass adequately account for the turbulent transport and any waviness of the falling film.
2. Heat transfer by conduction and mass transfer by diffusion in the direction of solution flow are negligible.
3. Vapor pressure equilibrium exists between the vapor and the liquid at the interface.
4. No shear forces are exerted on the liquid by the vapor and the pressure gradients are negligible.
5. The thermo-physical properties of the falling film are constant.

Subject to the above assumptions, the species transport equation for LiBr with diffusion only in the Y direction and convection due to mass-average motion of the mixture along X and Y directions is

$$U\frac{\partial \omega_s}{\partial X}+V\frac{\partial \omega_s}{\partial Y}=\frac{\partial}{\partial Y}\left[(D+D_t)\frac{\partial \omega_s}{\partial Y}\right] \tag{A.1}$$

The various symbols are defined in the section under Nomenclature.

Similarly, the energy equation gives

$$U\frac{\partial T_s}{\partial X}+V\frac{\partial T_s}{\partial Y}=\frac{\partial}{\partial Y}\left[(\alpha+\alpha_t)\frac{\partial T_s}{\partial Y}\right] \tag{A.2}$$

The continuity equation gives

$$\frac{\partial U}{\partial X}+\frac{\partial V}{\partial Y}=0 \tag{A.3}$$

The momentum transport equation can be written as

$$\frac{\partial}{\partial Y}\left[(\upsilon+\upsilon_t)\frac{\partial U}{\partial Y}\right]+g=0 \tag{A.4}$$

The energy conservation equation for the counter-flow coolant is

$$m_c c_c\frac{dT_c}{dX}=-h_c(T_w-T_c) \tag{A.5}$$

The mass flow rate of the coolant is suitably normalized to the area of heat flow from the film to the coolant across the separating wall.

The above governing equations are cast in the dimensionless form using the following dimensionless variables

$$\begin{aligned}
&x=\frac{X}{\delta},\quad y=\frac{Y}{\delta},\quad \theta=\frac{T-T_{s,o}}{\Delta T},\\
&\phi=\frac{\omega-\omega_{s,o}}{\Delta\omega},\quad u=\frac{U}{U_m},\quad v=\frac{V}{U_m},\\
&Re=\frac{U_m\delta}{\upsilon},\quad Pr=\frac{\upsilon}{\alpha},\quad Pr_t=\frac{\upsilon_t}{\alpha_t},\quad Fr=\frac{U_m^2}{g\delta},\\
&Sc=\frac{\upsilon}{D},\quad Sc_t=\frac{\upsilon_t}{D_t},\quad \Delta T=T_e(\omega_{s,o})-T_{s,o},\\
&\Delta\omega=\omega_e(T_{s,o})-\omega_{s,o}
\end{aligned} \tag{A.6}$$

The conservation equations of species, energy and momentum Eqs. (A.1), (A.2) and (A.4) can be expressed in the following dimensionless form

$$u\frac{\partial \phi_s}{\partial x}+v\frac{\partial \phi_s}{\partial y}=\frac{1}{ReSc}\frac{\partial}{\partial y}\left[\left(1+\frac{Sc\upsilon_t}{Sc_t\upsilon}\right)\frac{\partial \phi_s}{\partial y}\right] \tag{A.7}$$

$$u\frac{\partial \theta_s}{\partial x}+v\frac{\partial \theta_s}{\partial y}=\frac{1}{RePr}\frac{\partial}{\partial y}\left[\left(1+\frac{Pr\upsilon_t}{Pr_t\upsilon}\right)\frac{\partial \theta_s}{\partial y}\right] \tag{A.8}$$

$$\frac{Fr}{Re}\frac{\partial}{\partial y}\left[\left(1+\frac{\upsilon_t}{\upsilon}\right)\frac{\partial u}{\partial y}\right]+1=0 \tag{A.9}$$

The energy equation of the coolant becomes

$$\frac{d\theta_c}{dx}=-\left(\frac{h_c\delta}{m_c c_c}\right)(\theta_w-\theta_c) \tag{A.10}$$

A.1. Stream-wise mean velocity and relationship for Fr/Re

Integrating the momentum Eq. (A.9) and applying the condition that the shear interface is zero gives the stream wise velocity gradient as

$$\frac{du}{dy}=\frac{Re(1-y)}{Fr(1+\upsilon_t/\upsilon)} \tag{A.11}$$

The mean velocity is given by

$$U_m\delta=\int_0^\delta U\,dY \tag{A.12}$$

Eq. (A.12) can be integrated by parts to obtain

$$U_m\delta = U(\delta)\delta - \int_0^\delta \left(\frac{dU}{dY}\right) Y\,dY \tag{A.13}$$

Substituting the dimensional form of Eq. (A.11) for the two terms on the RHS of Eq. (A.13) and rearranging the resulting equation the following expression is obtained for the mean velocity

$$U_m\delta = \int_0^\delta \frac{(g/\upsilon)(\delta - Y)^2}{(1+\upsilon_t/\upsilon)}\,dY \tag{A.14}$$

The dimensionless form of Eq. (A.14) gives the relation between Re and Fr as

$$\frac{Fr}{Re} = \int_0^1 \frac{(1-y)^2\,dy}{(1+\upsilon_t/\upsilon)} \tag{A.15}$$

A.2. Transverse velocity distribution

The transverse velocity distribution is obtained by integrating the continuity Eq. (A.3).

$$\text{Now} \quad \frac{\partial U}{\partial X} = \frac{\partial(uU_m)}{\partial X} = u\frac{\partial U_m}{\partial X} + U_m\frac{\partial u}{\partial X} \tag{A.16}$$

$$\text{But} \quad U_m\frac{\partial u}{\partial X} = U_m\frac{\partial u}{\partial y}\frac{\partial y}{\partial X} = U_m\frac{\partial u}{\partial y}\left[-\frac{Y}{\delta^2}\right]\frac{d\delta}{dX} \tag{A.17}$$

$$\text{Therefore,} \quad \frac{\partial U}{\partial X} = u\frac{\partial U_m}{\partial X} - \frac{yU_m}{\delta}\frac{d\delta}{dX}\frac{\partial u}{\partial y} \tag{A.18}$$

From Eqs. (A.3) and (A.18) it follows that

$$\frac{\partial v}{\partial y} = y\frac{d\delta}{dX}\frac{\partial u}{\partial x} - \frac{u\delta}{U_m}\frac{\partial U_m}{\partial X} \tag{A.19}$$

Two additional relations are useful in the integration of Eq. (A.19) to compute the velocity distribution. These are obtained by applying overall mass conservation across a section of the film.

$$\Gamma = \rho_s U_m\delta \quad \text{and} \quad m_{abs} = \frac{d\Gamma}{dX} \tag{A.20}$$

Substituting from Eq. (A.20) in Eq. (A.19)

$$\frac{\partial v}{\partial y} = \left[u + y\frac{\partial u}{\partial y}\right]\frac{d\delta}{dX} - \frac{m_{abs}\delta u}{\Gamma} \tag{A.21}$$

Integrating Eq. (A.21) and applying the condition that $v = 0$ at $y = 0$ the velocity distribution is obtained as

$$v = yu\frac{d\delta}{dX} - \left[\frac{m_{abs}\delta}{\Gamma}\right]\int_0^y u\,dy \tag{A.22}$$

The detailed manner in which Eq. (A.22) is used in the numerical computation is explained in a later section.

A.3. Eddy transport coefficients

The various eddy transport coefficients to be used for falling films was investigated in detail by Yuksel and Schlunder [7] who compared the accuracy of the different models available in the literature.

(i) Near wall region ($0 \leqslant y \leqslant 0.6$)
The following expression [7] is used for the near wall region

$$\frac{\upsilon_t}{\upsilon} = \frac{1}{2}\left(-1 + \left\{1 + 0.64\frac{(yRe)^2}{Fr}(1-y) \times \left[1 - \exp\left(\frac{yRe}{a\sqrt{Fr}}\right)\right]^2 f^2\right\}^{1/2}\right) \tag{A.23}$$

where

$$f = \exp(-3.33y) \quad \text{and} \quad a = 25.1 \tag{A.24}$$

(ii) Core region ($0.6 \leqslant y \leqslant y_s$)
In the core region the value of $\frac{\upsilon_t}{\upsilon}$ is assumes to be the same as the value at $y = 0.6$ obtained from Eq. (A.23).

(iii) Surface region ($y_s \leqslant y \leqslant 1$)
Near the surface for $Re < 400$, the expression [7] is

$$\frac{\upsilon_t}{\upsilon} = 0.0158Re(1-y)^2 \tag{A.25}$$

For $Re \geqslant 400$ the near surface value is computed using the expression [7]

$$\frac{\upsilon_t}{\upsilon} = 8.31\times10^{-17}\frac{We}{Ka^{4/3}}(4Re)^{2n}(1-y)^2 \tag{A.26}$$

where $n = 695\upsilon^{1/2}$.

The boundary of the surface region, y_s is obtained by equating the RHS of Eqs. (A.25) or (A.26) to the value of $\frac{\upsilon_t}{\upsilon}$ in the core region.

Following Yuksel and Schlunder [7], the turbulent Prandtl number is assumed constant over the film and equal to 0.9. The turbulent Schmidt number assumed to be equal to the turbulent Prandtl number.

A.4. Boundary conditions and heat and mass transfer coefficients

The boundary conditions are as follows:

At the interface, $Y = \delta$

The mass flux is given by

$$m_{abs} = -\frac{\rho_s D}{\omega_{if}}\frac{d\omega_s}{dY} \tag{A.27}$$

The heat flux is given by

$$q_{abs} = m_{abs}i_{ab} = k_s\frac{dT_s}{dY} \tag{A.28}$$

The vapor–liquid interface is assumed to at equilibrium corresponding to the pressure of the system. Assuming the equilibrium condition to be linear [3]

$$\omega_{if} = a + bT_{if} \tag{A.29}$$

where the constants a and b depend on the pressure of the system.

At the wall, $Y = 0$

$$T_w(X) = T_s(X,0), \quad \frac{d\omega_s}{dY} = 0 \quad \text{and}$$

$$k_s \frac{dT_s}{dY} = h_c(T_s(0) - T_c) \tag{A.30}$$

The entry conditions for the falling-film and counter-flow-coolant are:

$$\text{At } X = 0, \quad T_s(0,Y) = T_{s,o} \text{ and } \omega_s(0,Y) = \omega_{s,o} \tag{A.31}$$

$$\text{At } X = L, \quad T_c = T_{co} \tag{A.32}$$

The dimensionless forms of the boundary conditions are as follows:

$$\text{At } y = 1, \quad \frac{d\phi_s}{dy} = -\frac{m_{abs}(\Delta\omega\phi_{if} + \omega_{s,o})}{\rho_s D \Delta\omega} \tag{A.33}$$

$$\frac{d\theta_s}{dy} = \frac{m_{abs} i_{ab} \delta}{k_s \Delta T} \tag{A.34}$$

The interface equilibrium condition Eq. (A.29) becomes

$$\phi_{if} = 1 - \theta_{if} \tag{A.35}$$

$$\text{At } y = 0, \quad \theta_w(x) = \theta_s(x,0), \quad \frac{d\phi_s}{dy} = 0 \quad \text{and}$$

$$\frac{d\theta_c}{dy} = \left(\frac{h_c \delta}{k_s}\right)(\theta_s(0) - \theta_c) \tag{A.36}$$

The entry conditions Eqs. (A.31) and (A.32) become

$$\text{At } x = 0, \quad \theta_s(0,y) = 0 \quad \text{and} \quad \omega_s(0,y) = 0 \tag{A.37}$$

$$\text{At } x = \frac{L}{\delta}, \quad \theta_c = \theta_{co} \tag{A.38}$$

The present numerical model will be used to extract the heat and mass transfer coefficients from the interface to the bulk liquid h_o and k_m respectively and the heat transfer coefficient from the bulk liquid to the wall h_i. These transfer coefficients are used in the development of the simplified model outlined in Section 2.

A.5. Computational procedure

The thickness of the falling film increases due to the absorption of vapor at the interface. The variation of the film thickness is taken account by using the coordinate transformation used by Choudhary et al. [5]. Using the staggered grid with denser mesh at the interface region, an upwind scheme is adopted to solve the species and energy transport Eqs. (A.7) and (A.8). Numerical accuracy for the mass fluxes and temperatures are set at 5×10^{-8} and 10^{-4} respectively.

References

[1] J.D. Killon, S. Garimella, A critical review of models of coupled heat and mass transfer in falling-film absorption, Int. J. Refrig. 24 (2001) 755–797.

[2] G. Grossman, Simultaneous heat and mass transfer in film absorption under laminar flow, Int. J. Heat Mass Transfer 6 (3) (1983) 357–371.

[3] G.A. Ibrahim, G.A. Vinnicombe, A hybrid method to analyse the performance of falling film absorbers, Int. J. Heat Mass Transfer 36 (5) (1993) 1383–1390.

[4] B.J.C. van der Wekken, R.H. Wassenaar, Simultaneous heat and mass transfer accompanying absorption in laminar flow over a cooled wall, Int. J. Refrig. 11 (1988) 70–77.

[5] S.K. Choudhury, D. Hisajima, T. Ohuchi, A. Nishiguchi, T. Fukushima, S. Sakaguchi, Absorption of vapors into liquid films flowing over cooled horizontal tubes, ASHRAE Trans. 99 (2) (1993) 81–89.

[6] Gershon Grossman, Michael T. Heath, Simultaneous heat and mass transfer in absorption of gases in turbulent liquids, Int. J. Heat Mass Transfer 27 (12) (1984) 2365–2376.

[7] M.L. Yuksel, E.U. Schlunder, Heat and mass transfer in non-isothermal absorption of gases in falling liquid film. Part II: theoretical description and numerical calculation of turbulent falling film heat and mass transfer, Chem. Eng. Process 22 (1987) 203–213.

[8] M.L. Yuksel, E.U. Schlunder, Heat and mass transfer in non-isothermal absorption of gases in falling liquid film. Part I: experimental determination of heat and mass transfer coefficients, Chem. Eng. Process 22 (1987) 193–202.

[9] Vikas Patnaik, H. Perez-Blanco, A study of absorption enhancement by wavy film flows, Int. J. Heat Fluid Flow 17 (1996) 71–77.

[10] V. Patnaik, H. Perez-Blanco, A counter flow heat-exchanger analysis for the design of falling film absorbers, Int. Absorption Heat Pump Conf. AES-31 (1993) 209–216.

[11] V. Patnaik, H. Perez-Blanco, W.A. Ryan, A simple analytical model for the design of vertical tube absorbers, ASHRAE Trans. 99 (2) (1993) 69–80.

[12] A.T. Conlisk, The use of boundary layer techniques in the design of a falling film absorber, Int. Absorption Heat Pump Conf. AES-31 (1993) 163–170.

[13] W.A. Ryan, Water absorption in an adiabatic spray of aqueous Lithium Bromide solution, Int. Absorption Heat Pump Conf. AES-31 (1993) 155–162.

[14] Tsai Bor-Bin, H. Perez-Blanco, Limits of mass transfer enhancement in lithium bromide–water absorbers by active techniques, Int. J. Heat Mass Transfer 41 (1998) 2409–2416.

[15] J.W. Andberg, G.C. Vliet, A simplified model for absorption of vapors into liquid films flowing over cooled horizontal tubes, ASHRAE Trans. 93 (2) (1987) 2454–2466.

[16] H. Uddholm, F. Settewall, Model for dimensioning a falling film absorber in an absorption heat pump, Int. J. Refrig. 11 (1988) 41–45.

[17] W.A. Miller, M. Keyhani, The correlation of simultaneous heat and mass transfer experimental data for aqueous lithium bromide vertical falling film absorption, J. Solar Energy Eng. 123 (2001) 30–42.

[18] S.M. Deng, W.B. Ma, Experimental studies on the characteristics of an absorber using LiBr/H_2O solution as working fluid, Int. J. Refrig. 22 (1999) 293–301.

[19] W.A. Miller, H. Perez-Blanco, Vertical-tube aqueous LiBr falling film absorption using advanced surfaces, Int. Absorption Heat Pump Conf. AES-31 (1993) 185–202.

[20] Md. Raisul Islam, N.E. Wijeysundera, J.C. Ho, Evaluation of heat and mass transfer coefficients for falling-films on tubular absorbers, Int. J. Refrig. 26 (2003) 197–204.

[21] Md. Raisul Islam, N.E. Wijeysundera, J.C. Ho, Simplified models for coupled heat and mass transfer in falling-film absorbers, Int. J. Heat Mass Transfer 47 (2) (2004) 395–406.

[22] W. Keys, M. Crawford, B. Weigand, Convective Heat and Mass Transfer, McGraw-Hill, New York, 2005.

[23] W.A. Miller, The experimental analysis of aqueous lithium bromide vertical falling film absorption, Ph.D. thesis, University of Tennessee, Knoxville, 1998.

[24] R. Yang, D. Jou, Heat and mass transfer on the wavy film absorption process, Can. J. Chem. Eng. 71 (1993) 533–538.